Journal of Arid Environments 225 (2024) 105245

Contents lists available at ScienceDirect

Journal of Arid Environments

journal homepage: www.elsevier.com/locate/jaridenv

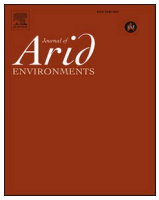

Thinning relationships of woody encroachers in a US southwestern shrubland

Trevor Roberts *, Niall P. Hanan

Plant and Environmental Sciences, New Mexico State University, Las Cruces, NM, USA

ARTICLE INFO

Keywords:
Woody encroachment
Lidar
Jornada basin
Competition
NAIP
Thinning

ABSTRACT

Woody plant encroachment degrades the economic and environmental potential of drylands by altering processes such as nutrient fluxes, ecohydrology, and ecosystem services. Though past research has investigated the encroachment process, relatively little is known about post-encroachment shrub community ecology. To better quantify dynamics within post-woody encroachment shrub communities, we combined USGS lidar height data and multispectral imagery to estimate shrub density, shrub height, shrub cover, and shrub volume across the Jornada Basin Long Term Ecological Research (JRN-LTER) site in southern New Mexico, USA. Structural estimates were analyzed in search of telltale signs of community competition, specifically, the presence of thinning relationships. Results demonstrated density-dependent thinning relationships in shrub communities of creosote and mesquite, indicating a large role for competition in arid shrub communities even at relatively low shrub densities and cover (~35% cover). In addition, shrub volume estimates better modeled the expected thinning dynamics of shrub communities than shrub canopy cover measurements. Overall, our results indicate the utility of lidar data in extending two-dimensional descriptions of woody vegetation structure (i.e., woody canopy cover) into the critical third dimension (i.e., woody plant volume), as well as the relative importance of competition and demographic bottlenecks to vegetation structure in drylands.

1. Introduction

Woody plant encroachment (WPE) threatens the structure and function of ecosystems across the world (Archer et al., 2017; Maestre et al., 2016). WPE affects diverse ecosystems, but encroachment in arid and semi-arid rangelands receives special focus given the elevated sensitivity of these regions to ecological perturbations. Furthermore, arid and semi-arid rangelands are widely relied on for livestock production and wildlife, and are thus important to the economic wellbeing of many communities (Black et al., 2021; Huang et al., 2017; Reid et al., 2014). WPE alters various ecological processes within arid and semi-arid systems, including changes to carbon sequestration potential, ecohydrology, and ecosystem services such as forage production, among others (Archer et al., 2017; Wilcox et al., 2022). Taken together, these facts indicate the need to further study the dynamics and spread of woody plants in arid and semi-arid ecosystems, lest the beneficiaries of such systems suffer.

Many arid and semi-arid drylands across the world have experienced widespread WPE over the last 150 years (Goslee et al., 2003; Wilcox et al., 2022), largely due to perturbations from overgrazing and climate change in the form of periodic drought (D'Odorico et al., 2012). In the US southwest, for example, historic grasslands are now dominated by shrub communities (Duniway et al., 2018). In general, WPE has led to regime shifts in areas historically dominated by C_4 grasses, reducing grass cover and degrading many of the ecosystem services relied on by local ranchers and communities (Bestelmeyer et al., 2015; Duniway et al., 2018; Saco et al., 2018).

Given the economic consequences of grassland to shrubland regime shifts in arid rangelands, substantial prior research has investigated inter-specific interactions between woody and herbaceous plants (Buffington and Herbel 1965; Christensen et al., 2021; Duniway et al., 2018), and, more specifically, the onset and propagation of WPE (Archer et al., 2017). However, as woody plants have come to dominate landscapes, relatively little research has investigated the effects of intra-specific (or intra-functional group) interactions between woody plants, or, in other words, the community ecology of shrublands post-woody encroachment. Sea and Hanan (2012) and Dohn et al. (2017) demonstrated the importance of self-thinning and shrub-shrub

* Corresponding author.
E-mail address: throberts@wisc.edu (T. Roberts).

https://doi.org/10.1016/j.jaridenv.2024.105245
Received 18 December 2023; Received in revised form 22 July 2024; Accepted 23 August 2024
Available online 30 August 2024

competition in dryland woody populations in Africa, and, more recently, similar research has unearthed the importance of thinning within the *P. glandulosa* and *L. tridentata* populations of the Jornada Basin in southern New Mexico, USA (Ji et al., 2019; Wojcikiewicz et al., 2024), but these studies are unique in the woody encroachment literature. We suggest building on these previous studies, and that self-thinning and shrub-shrub competition may be an important process controlling vegetation structure in US southwestern drylands.

Shrub-shrub competition and self-thinning generate predictable changes in woody plant density and size, namely, a tradeoff between a greater number of individuals and their respective sizes (Fig. 1; Aschehoug et al., 2016; Hatton et al., 2019). The thinning process is visible in graphs of density and size, forming what is often called a thinning line. Thinning lines are assumed to represent values of population density and size at which resource limitations are exceeded, such that additional recruitment of young shrubs and the growth of adult shrubs is limited (i.e., the population "carrying capacity"; Archer et al., 2017). Because plant communities above the thinning line exceed resource capacity, they must either decrease in number (density) or average size to fall below it (i.e., return to carrying capacity; Fig. 1). Importantly, carrying capacities differ between regions in response to variability in rainfall and soils (Axelsson and Hanan 2017), and between populations in response to local-scale biotic and edaphic variability (Sayre et al., 2012). Therefore, thinning lines are often indicative of underlying community function and resource use (Taki et al., 2010; Urgoiti et al., 2023). In drylands, for example, water is typically the most limiting resource to plant recruitment and growth, such that thinning relationships implicate competition for limited water (Axelsson and Hanan 2018). We anticipate that thinning lines will provide new insight into maximum potential shrub size and density, serve as an accurate indicator of competition among shrubs, and respond to variable geomorphic templates and shrub species dominance patterns (Fig. 2).

Thinning line slopes (i.e., thinning coefficients) represent the tradeoff between vegetation density and size in terms of population-scale resource demand. Previous studies suggest that thinning line slopes range from −1 to −4/3 when plotted on log-log axes (Belgrano et al., 2002; Sea and Hanan 2012). Thinning line slopes and intercepts differ according to taxa, environmental condition, and–critical for this study–the metric adopted to quantify plant size, creating substantial confusion in their application. Despite the complexity of thinning coefficients, it is possible to posit specific slopes under certain conditions. A thinning slope of −1, for example, is expected in plant communities at carrying capacity such that mean size * density = resource capacity (Yu et al., 2024). Such plant communities make complete use of their available resources, so any increase in the density of the community necessitates an equivalent decrease in average size (Fig. 1). Because we expect dense shrublands in the Jornada Basin to be at carrying capacity (i.e., equilibrium, complete use of available resources), thinning slopes should equal −1 (Sea and Hanan 2012). For example, if our vegetation size metric is mean volume, then a fitted thinning line of −1 in a log-log plot of mean size against density is a line of equal community volume (i.e., mean volume * density = resource capacity), suggesting a strong relationship between vegetation volume and population-level resource use across all values of vegetation size and density. Importantly, this method relies on the principle that the vegetation metric most proximal to underlying resource use will return a thinning slope of −1, such that, in this context, differences in thinning relationships between metrics are due to the relative ability of metrics to quantify the operative components of vegetation rather than biological differences based on thinning more broadly. With this logic in mind, multiple metrics of shrub structure may be compared to test for proportionality to water-limited, competition-based thinning, and evaluated for which metric provides slopes closer to −1 (Fig. 1).

Although past research has discovered thinning lines in arid shrublands using two-dimensional size metrics (e.g., canopy area; Ji et al., 2019), for the purposes of indexing resource use, we contend that a three-dimensional size metric (e.g., canopy volume) should better illustrate thinning relationships. Leaf area index (LAI) is most often used to relate vegetation characteristics to transpiration (Schmidt-Walter et al., 2014; Stockle 1992), but LAI estimates at the fine grain needed to study shrub communities were unavailable to us. We hypothesize that canopy volume should better reflect vegetation resource use (and subsequent community processes like thinning) than canopy area. This is because canopy area ignores shrub height as a critical dimension defining the size and resource use of an individual shrub. Canopy volume, by contrast, includes height information and, as such, is likely to be a superior index of total leaf area (i.e., LAI), sap flow, and water resource use (Fig. 1).

Measurements of density, canopy area, and canopy volume are difficult to obtain at large spatial extents using field sampling methods. Drylands are structurally heterogenous at multiple spatial scales (Sayre et al., 2012), necessitating the use of landscape scale observations to yield generalizable conclusions. Consequently, remote sensing instruments provide the most obvious method by which to sample the

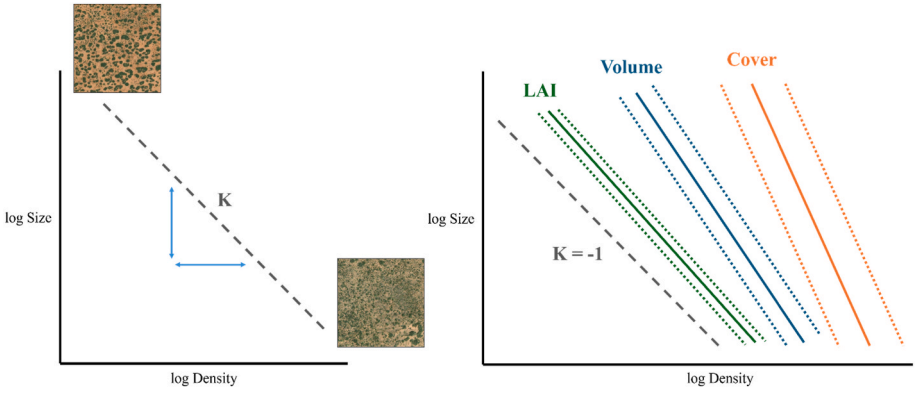

Fig. 1. Conceptual figure of thinning line slope expectations (A) and vegetation metrics (B). (A) In a population maximizing resource use, thinning lines approximate carrying capacity (K), such that any increase in the number of individuals must result in an equivalent reduction in the average size of individuals. This 1:1 reduction results in our expectation of thinning lines of slope −1. Populations can either emerge with fewer, larger individuals (top photo) or more, smaller individuals (bottom photo), both of which are visible in the arid shrublands of the US southwest. (B) Multiple metrics of shrub size can be compared to the −1 slope expectation by plotting their thinning lines. Metrics of size that better represent vegetation resource capture should more closely approach the −1 slope in populations at carrying capacity. In this example, we anticipate that leaf area index (LAI) will closely approximate −1, while volume will be slightly worse, and canopy cover will be worse than volume. Similarly, confidence intervals for fitted thinning slopes should be narrower for more proximal metrics. Note that thinning lines in (B) are arbitrarily offset along the x-axis for visualization of slopes and confidence intervals.

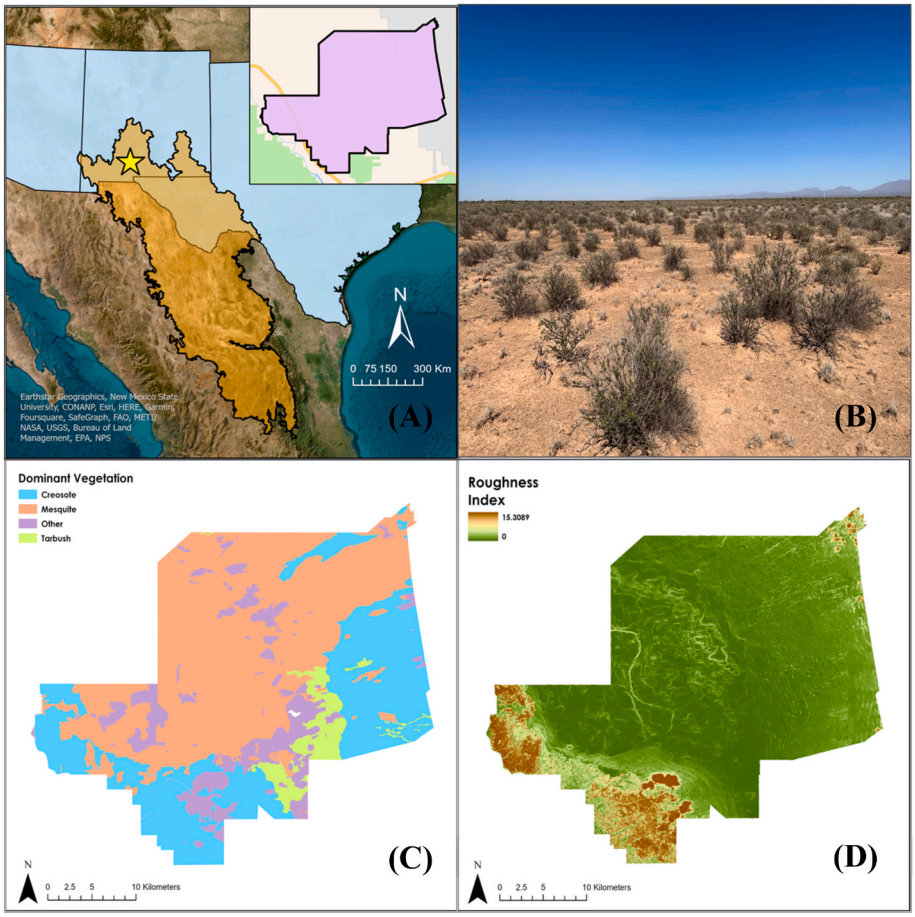

Fig. 2. Location and characteristics of the Jornada Basin study area. (A) The position of the Jornada in the greater Chihuahuan Desert and southern New Mexico, USA, (B) Example tarbush (*F. cernua*) species shrubland in the JRN-LTER; (C) Map of the Jornada Basin showing dominant shrub species (adapted from Gibbens et al., 2005), and (D) Topographic roughness map of the Basin (derived from USGS DEM).

spatial variability of dryland plant populations. Multiple remote sensing products aimed at quantifying landscape scale cover and productivity exist, but most of these products fail to resolve individual shrub canopies (Allred et al., 2021; Jones et al., 2021). Therefore, the task of appropriately measuring plant density and size at landscape scale requires a combination of fine spatial resolution and wide spatial extent. Ji et al. (2019) created a fine-grained (1 m) shrub map of the Jornada Basin by applying a neural network approach to imagery from the National Agriculture Imagery Program (NAIP). The map of Ji et al. (2019) provides the canopy area of shrub patches in the Jornada Basin, but fails to integrate height information. In this study, we use airborne lidar measurements to explore how addition of the critical third dimension provides insight into self-thinning processes of arid shrublands.

We hypothesize that lidar-based heights, when fused with canopy cover data to estimate shrub volumes, will better index total leaf area and water resource use of shrubs than canopy area measurements. Therefore, volume-based thinning lines should have slopes closer to −1 than those derived from canopy area measurements. This work will extend earlier inference of density-dependent competition among shrubs of the Jornada Basin (Wojcikiewicz et al., 2024), and will illuminate the importance of selecting size metrics related to underlying resource limitation which, in drylands, is typically water. In this context, shrub volume is likely to be more closely related to transpiring leaf area than is canopy diameter or area (Liu et al., 2021). Finally, if shrub volume-based thinning occurs, it will reinforce our understanding of intraspecific (or intra-plant functional type) competition in limiting woody populations in drylands, as well as demonstrate the value of three-dimensional lidar products in quantifying woody plant community structure and resource use.

2. Methods

2.1. Study area

The Jornada Basin Long Term Ecological Research site (JRN-LTER) is a 104,166 ha research site located in the northern Chihuahuan Desert in southern New Mexico, USA (Fig. 2). The site is managed by the USDA Agricultural Research Service and New Mexico State University, incorporating the 78,266 ha Jornada Experimental Range (JER) and the 25,900 ha Chihuahuan Desert Rangeland Research Center (CDRRC). The site is characterized by high aridity, significant solar inputs, and severe water limitation across most of the year. The average maximum temperature is 36 °C in June and 13 °C in January. Average precipitation is 230 mm per year, with over half of rainfall occurring in the brief monsoon season between July 1st and October 1st (Greenland et al., 1997). The San Andres Mountains occupy the eastern edge of the JRN-LTER. Due to complex topography and differences in vegetation and climate in the eastern San Andres mountains, they are excluded from our analysis.

Historically, *Bouteloua eriopoda (*black grama) *and Pleuraphis mutica* (tobosa) grasslands predominated across the Jornada, but overgrazing and drought in the early and mid-20th Century resulted in plant community shifts toward woody species (Buffington and Herbel 1965; D'Odorico et al., 2012). Presently, *P. glandulosa* (honey mesquite), *L. tridentata* (creosote bush), and *Flourensia cernua* (tarbush) dominate across most of the Basin. Remnant black grama grasslands and other

grass species (*Scleropogon brevifolius* (burrograss), *Sporobolus* spp. (dropseeds)) persist in some areas, with small areas dominated by other shrub species, including *Atriplex canescens* (saltbush), *Ephedra* spp. (Mormon tea), and Yucca spp. (e.g., soaptree yucca), among others (see https://jornada.nmsu.edu/data-catalogs/species/lter-plants for complete list of JRN-LTER species). WPE in the JRN-LTER degraded many of the ecosystem services relied on by local communities (Bestelmeyer et al., 2015; Duniway et al., 2018; Saco et al., 2018). These impacts of WPE within the JRN-LTER are indicative of WPE in arid and semi-arid rangelands elsewhere, making the site ideal for study (Havstad et al., 2006).

We mostly focused on two shrub species typical of the Jornada Basin, honey mequite (*P. glandulosa*) and creosote bush (*L. tridentata*). Both species are long-lived, desert-adapted plants. Honey mesquite grows in multiple forms depending on climate and land history but is typically shrub-like in the JRN-LTER (Meyer 1971). Creosote bush is similar but tends to grow smaller and in denser stands (Peters and Gibbens 2006). Unlike creosote bush, honey mesquite produces distinctive dunes in some areas of the Jornada Basin (Duniway et al., 2018). Shrub sizes vary in the Jornada Basin, but few shrubs grow taller than 2 m in height, except for patches of the coppice dune producing mesquite (Duniway et al., 2018; Peters and Gibbens 2006). Previous research has found that average shrub cover at 1 ha scale ranges from 3% to 27% and average patch density ~120 to 350 patches, depending on landform (Ji et al., 2019). Rates of WPE have slowed in recent decades compared to those seen in the 20th century, creating a landscape with relatively static patterns of woody plants (Gibbens et al., 2005; Huang et al., 2018; Wojcikiewicz et al., 2024).

2.2. Shrub cover data and processing

Shrub cover data were extracted from an update of the shrub canopy mapping products of Ji et al. (2019). The original data were created by applying a neural network approach to NAIP imagery from 2011, but contained a void in predictions in their center due to terrain complexity reducing local shrub canopy mapping efficacy. In this study we filled the void by merging the original map with a regional analysis (see https://doi.org/10.6073/pasta/313fec8669bc7b4d8debf7393dd26c1f). As much of the original map was used as possible to facilitate comparison of this study's results to those of Ji et al. (2019). The merged shrub map was aggregated to 1 ha scale, re-projected to a common spatial reference system also used for the volume and density maps (see below), then clipped to the extent of the JRN-LTER. Cover data in topographically rough areas were removed due to lidar data limitations (see below for more detail).

2.3. Shrub volume data and processing

Light detection and ranging (lidar) point clouds were downloaded from the USGS 3D Elevation Program (3DEP) data portal (https://apps.nationalmap.gov/downloader/). Data met or exceeded USGS quality level 2 standards (<19.6 cm non-vegetated vertical accuracy at 95% confidence) and were already geo-rectified, quality controlled, and classified into ground, noise, water, and other. The "other" class was considered vegetation. Data were clipped to encompass the JRN-LTER study area.

Lidar missions were conducted in October of 2019. Although the gap between lidar and NAIP data collection (2019 vs. 2011) may have introduced some error in shrub position between analyzed products, dramatic landscape change in the JRN-LTER has not occurred since the 20th century (D'Odorico et al., 2012; Havstad et al., 2006). In recent decades, shrublands in the JRN-LTER and similar systems have remained relatively static (i.e., slowing WPE; Huang et al., 2018), minimizing concern regarding use of temporally mismatched data products.

Lidar data were processed in R software using the sf and lidR packages (Pebesma 2018; R Core Team 2021; Roussel et al., 2020). Lidar returns flagged as overlapping between two or more point clouds were removed and resulting point cloud tiles were height normalized using a triangular irregular network to approximate the ground surface. Points classified as other, but that were less than 50 cm above the ground, were dropped. This minimum height filter excluded seedlings and smaller shrubs from subsequent analysis, but reduced confusion with most herbaceous plants, which are generally <50 cm in the Jornada Basin. In addition, lidar returns above 10 m were excluded to prevent erroneous returns from inflating average shrub height estimates. These filtering steps resulted in an average point density of 0.1 per m^2. Due to this sparse point density, heights of all individual shrubs could not be determined. Instead, we considered the lidar height returns as samples of shrub heights at hectare-scales and subsequent processing steps aggregated and averaged lidar data to address this fact. Next, height filtered and normalized point clouds were converted into raster format canopy height models using the points2raster algorithm in the lidR package. Raster data were processed in R using the terra package (Hijmans 2022). As stated above, the smoothed CHM was aggregated to estimate mean heights at a resolution of 1 ha (100 × 100 m). Finally, the 1 × 1 m shrub map of Ji et al. (2019) was multiplied against the CHM to estimate shrub volumes across the Jornada Basin at 1 ha resolution (Fig. 4). Although this approach was limited by its abstraction of canopy geometry into hectare-scale grid cells, it allowed for the inclusion of the critical vertical height dimension in shrub structure estimates rather than relying only on 2-dimensional canopy cover measurements.

Lidar instruments often struggle to resolve vegetation heights in topographically rugged areas, especially when point density is sparse such as in our approach (Kulawardhana et al., 2017). To combat this issue, a roughness surface derived from the USGS DEM of the region was used to mask out shrub volume estimates in especially rugged regions of the JRN-LTER (Fig. 2). Areas with roughness index values greater than 1 corresponded to the mountainous and escarpment regions of the JRN-LTER, and were thus masked on the shrub map. This roughness mask was also applied to the cover and density map to better align cover, density, and volume estimates.

2.4. Shrub density data and processing

Shrub density data were, like shrub cover, extracted from the merged shrub map of Ji et al. (2019). Although density, cover, and volume were all extracted from the same base shrub map product of Ji et al. (2019), though only partially for volume, they each represent distinct enough interpretations of the underling aerial imagery that circularity should not have caused any issues in our analysis. Remote sensing analyses commonly use the same imagery to quantify multiple vegetation attributes and the relationships between them without losses in accuracy or research applicability (e.g., Carrasco et al., 2019; Goslee et al., 2003).

Next, the merged shrub map was cropped into 9 sections of equal area to ease computational load. Subsequent raster processing was coded in the stars package rather than the terra package due to stars' more efficient handling of large raster files (Pebesma 2021). The 9 cropped shrub map sections were vectorized using the "st_as_sf" function in the sf package. Centroids of these vectors were computed, then the 9 sections of centroids were merged together. A map template corresponding to the 1 ha sections in the shrub volume and shrub cover maps was used to count the number of centroids in each hectare. Finally, this template was rasterized then clipped to the extent of the JRN-LTER, resulting in a map of shrub density per hectare spatially aligned to the volume and cover maps.

The shrub map of Ji et al. (2019) does not distinguish between shrub patches and shrub individuals. Given the 1 m spatial resolution of the shrub map, shrubs closer than ~1 m may be amalgamated into a single patch in the density map. Therefore, the shrub density map measures the number of shrub patches within a hectare area, not the number of individuals. This limitation in spatial resolution should not affect our

thinning line analysis since any systematic reduction in shrub density will be compensated by an increase in mean shrub size.

2.5. Shrub data synthesis

Shrub volume, cover, and density surfaces were combined and co-registered in a single data structure. Finally, data were cleaned and exported using tidyverse tools (Roberts and Hanan 2023; Wickham et al., 2019).

2.6. Statistical analysis

95th quantile regression was applied to volume, cover, and density estimates using the quantreg package in R (Koenker 2022). Quantile regression allows for the reduction of residuals around a specified quantile of the dependent variable as opposed to the mean (Koenker 2022). Because significant density-dependent competition is only expected at high densities, quantile regression is a more appropriate tool to model thinning processes compared to ordinary least squares linear regression. Two 95th quantile regression models were created, one predicting log10 average shrub cover with log10 density, and the other predicting 1og10 average shrub volume with log10 density. Model slopes were compared to the −1 expectation. Finally, model predictions were plotted atop the data using the ggplot2 package in R (Wickham et al., 2019).

2.7. Shrub species-specific analysis

Because spatial patterns in the density, cover, and volume maps appeared to align with topography and species distributions, maps were compared to a shrub species distribution map (Gibbens et al., 2005) and a DEM-derived topographic roughness map of the Jornada Basin (Fig. 2). Species were separated in the thinning line analysis by applying the species distribution map (Gibbens et al., 2005) to the density, cover, and volume maps (Fig. 3). Hectare grid cells with >50% dominance of creosote or mesquite were assigned their respective dominant species class. All other cells were labeled "other."

3. Results

3.1. Shrub maps

Fig. 3 shows the shrub density, shrub height, shrub cover, and shrub volume maps. Each map encompasses the entirety of the Jornada Basin minus regions masked due to topographic roughness. The density map demonstrates an average density of approximately 192 shrubs per hectare (Table 1). The spatial arrangement of density correlates with vegetation type (Fig. 4), with regions of creosote bush (297 ± 137 patches/ha) often having much higher density than mesquite (170 ± 83.3 patches/ha) or other shrub species, especially on the eastern edge of the JRN-LTER (Table 1; Fig. 3).

Two sharp lines are visible in the shrub density map oriented north-south and east-west on the eastern side of the Basin (Fig. 3). We initially hypothesized that these sudden changes in shrub density were associated with fence lines. Upon further analysis, however, it appears that the north-south line emerges due to aggregation from 1 m^2 scale to 1 ha along relatively steep elevation gradients, and where mesquite dominated communities on the sandy valley floor transition to creosote dominated communities of the piedmont. As such, the sharp edge is visible in the coarser-scale density map despite gradual changes in shrub density in the fine-scale data. On the other hand, the east-west line in the map's center is related to the merging of two iterations of the shrub

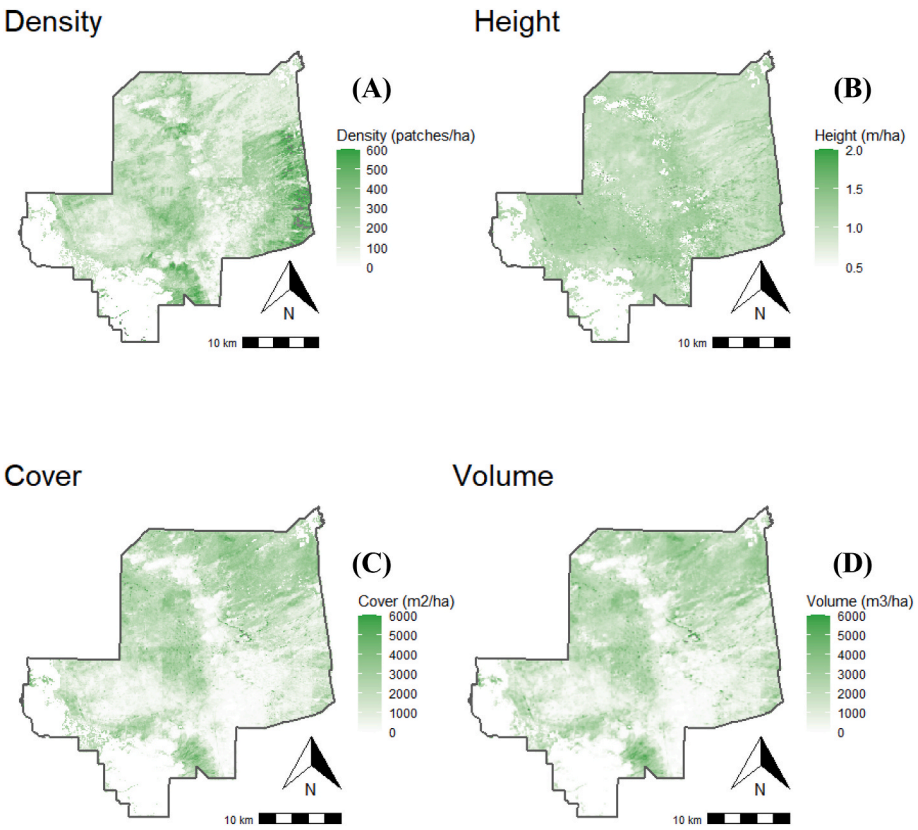

Fig. 3. Shrub metrics of the Jornada Basin. Shrub density (A), shrub height (B), shrub cover (C), and shrub volume (D) estimates, all at 1 ha spatial resolution. Maps were created by fusing lidar height estimates with canopy cover estimates obtained from multispectral airborne data. Areas of poor lidar performance due to topographic roughness are masked. The borders of the JRN-LTER extend further east than shown, but were not included due to mountainous terrain.

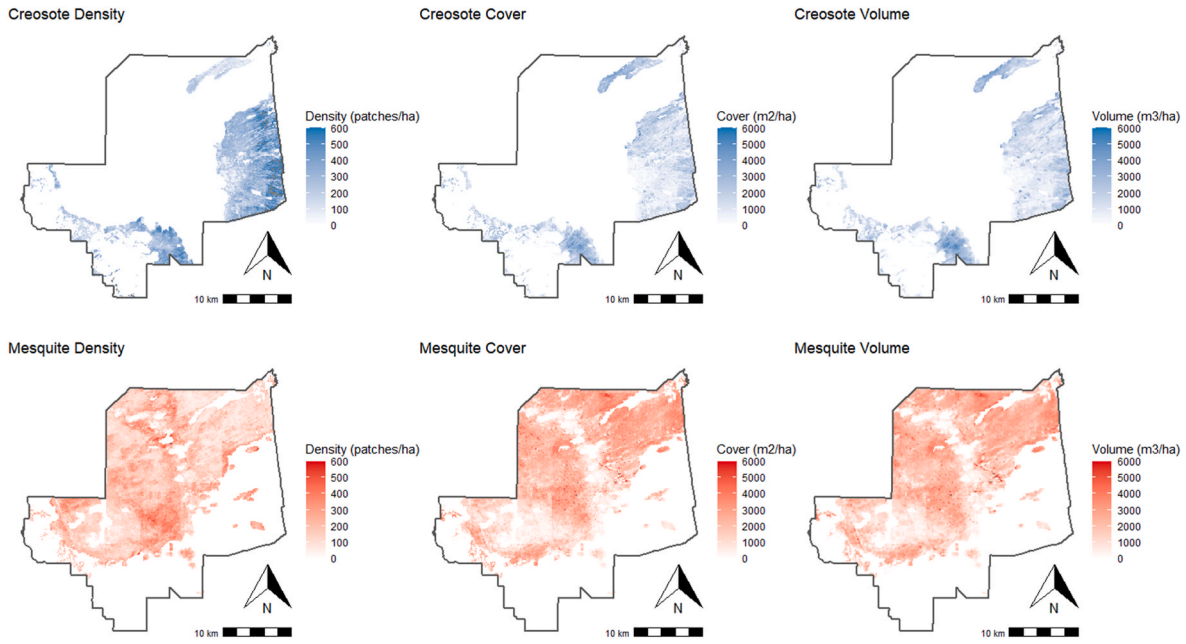

Fig. 4. Density, cover, and volume maps separated by creosote populations (above) and mesquite populations (below) in the JRN-LTER.

Table 1
Mean values of density, height, cover, and volume metrics across the Jornada Basin at 1 ha spatial resolution for creosote, mesquite, and global (all woody plants). Standard deviations of values provided in parentheses.

	Creosote	Mesquite	Global
Density (patches ha^{-1})	297 (137)	170 (83.3)	191.5 (119.63)
Height (m ha^{-1})	1.02 (0.144)	1.04 (0.155)	1.08 (0.28)
Cover (m^2 ha^{-1})	1442 (950)	1909 (987)	1557 (1081)
Volume (m^3 ha^{-1})	1446 (951)	1878 (895)	1559 (1051)

canopy products of Ji et al. (2019), with slight biases between their neural net predictions.

Shrub density and shrub volume show similar distributions. Maximum shrub cover and shrub volume occur at low to intermediate shrub density, implying that mean shrub size (i.e., canopy area, canopy volume, etc.) is at its highest where the number of shrubs is at its lowest (Fig. 3). The mean shrub cover across the JRN-LTER is approximately 1557 m^2/ha (i.e., 15.6%), though this value varies dramatically across the region (std. dev. = 1081 m^2/ha), and between creosote (1442 ± 950 m^2/ha) and mesquite (1909 ± 987 m^2/ha) dominated stands. Unlike density, shrub cover is generally low in the creosote-dominated piedmont (near the eastern edge of the site) and high in the central mesquite-

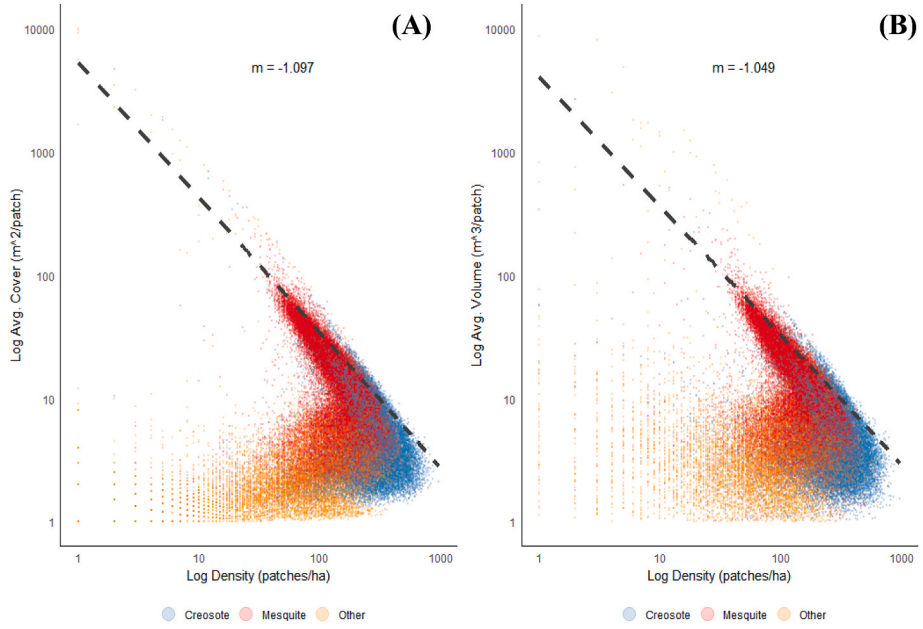

Fig. 5. Thinning lines of density-avg. cover (A) and density-avg. volume (B). Axes are log10 scaled. Thinning lines (dashed lines) are 95th quantile regression fits. Thinning line slopes are given. Confidence intervals are not shown due to their tight boundaries (CI cover: lower = −1.10, upper = −1.09; CI volume: lower = −1.06, upper = −1.04). Color represents shrub species. Note that the global 95th quantile regression appears to appropriately model both the creosote and mesquite populations.

dominated valley floor (Fig. 3). Thus, in general, shrubs either occur as populations of many, small individuals or fewer, large individuals. Furthermore, the relationship between cover and density appears to be somewhat species specific; Figs. 4 and 5 illustrate the tendency of mesquite to occur at lower densities and larger sizes than creosote.

The volume and cover maps are highly correlated ($r = 0.929$), in part because average shrub heights across much of the Jornada Basin are close to 1 m (mean = 1.08 m; std. dev = 0.28 m; Fig. 3). Still, the inclusion of vertical height information may improve the volume map's ability to discern thinning relationships among shrubs in the JRN-LTER, particularly the differences between creosote (average height = 1.02 ± 0.144 m) and mesquite (average height = 1.04 ± 0.155 m). The volume map demonstrates the same spatial, species-specific patterns as the cover map (Fig. 4). Across the entire Jornada Basin, mean shrub volume per hectare is ~1559 ± 1051 m^3/ha (creosote = 1446 ± 951 m^3/ha; mesquite = 1878 ± 895 m^3/ha), with a high degree of variability in shrub volumes across the Basin (std. dev. = 1051 m^3/ha).

3.2. Thinning lines

Shrub cover and shrub volume thinning lines on log-log axes are shown in Fig. 5. The log-log avg. cover-density 95th quantile regression provides highly significant coefficient estimates (slope = −1.097, $p < 0.001$). This slope estimate approaches the −1 expectation of thinning relationships. The avg. volume-density regression, however, returns coefficients closer to −1 (slope = −1.049, $p < 0.001$). Confidence intervals of the two slope estimates do not overlap, which, based on our hypothesis that the better index of shrub size will produce thinning lines closer to −1, suggests that shrub volumes provide modest but significant improvements in quantifying thinning relationships compared to cover (Fig. 5).

Mesquite and creosote populations separate across the thinning line, with mesquite trending toward lower densities and larger sizes and creosote trending to higher density with smaller sizes. Despite their separation in the thinning line point cloud, the proximity of regression coefficients to −1 implies that both species are well-modeled by the same thinning line (Fig. 5). Confidence intervals of species-specific quantile regressions corroborate that creosote and mesquite share thinning line slopes, at least with volume estimates, and that cover provides similar slopes (Fig. 6). On the other hand, slightly different intercepts between mesquite and creosote may suggest small differences in baseline resource-use efficiency between the two species, wherein creosote appears to sustain populations with higher cover and volume than mesquite. However, these intercepts extend far beyond realized values of volume and cover (Fig. 5; Fig. 6), and averages of actual values demonstrate that mesquite tends to grow larger than creosote (above). Other species in the JRN-LTER, meanwhile, do not occur along the thinning line in any significant number, tending to take smaller values of both density and size compared to creosote and mesquite.

4. Discussion

4.1. The thinning dynamic

Both the shrub cover and shrub volume thinning lines demonstrate the presence of density-dependent thinning in locations with larger and denser shrub populations, implying that additional shrub growth or establishment is limited by resource availability, presumably water availability in the arid conditions of the JRN-LTER. In theory, these limited resources provide a ceiling on potential shrub growth and establishment. In practice, however, precipitation variability likely leads to fluctuations in shrub growth, establishment, and mortality, such that the emergent thinning lines represent long-term average resource limitations, but with dynamics and lags in actual populations at shorter time-scales (Craine and Dybzinski 2013; Saco et al., 2018).

Theoretical considerations suggest that plant populations undergoing competitive self-thinning should thin at a rate ranging from −1 to −4/3, when size and density are both log-transformed (Belgrano et al., 2002; Hatton et al., 2019). However, thinning line slopes and intercepts are known to vary by site condition (Ge et al., 2017), and there remains considerable debate about expected slope values based on the conceptual framework used to produce them. Metabolic scaling theory, competition-density, and geometric versus fractal scaling theory all provide distinct predictions (Hatton et al., 2019; Vospernik and Sterba 2015; West et al., 1999). Vospernik and Sterba (2015), for example, found significant differences in thinning coefficients between species and based on estimation methods. Much of this confusion stems from varying assumptions and the specific measurements used to index size

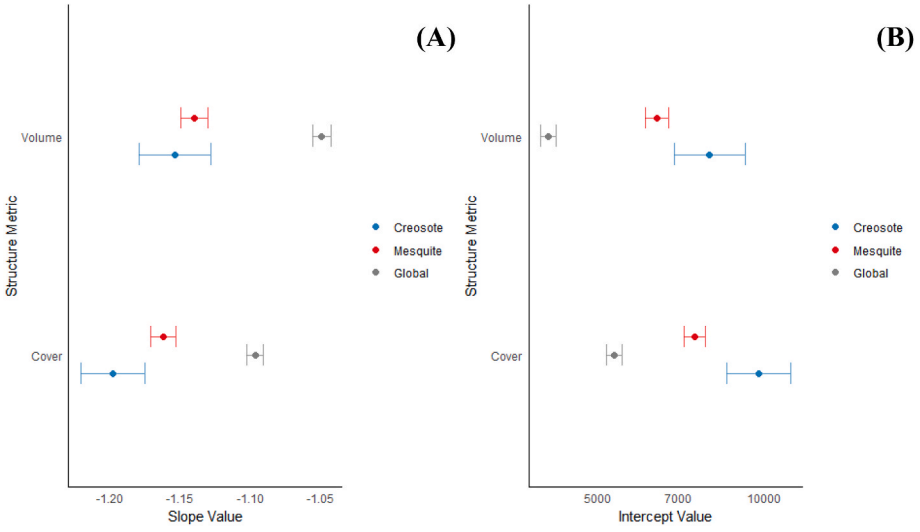

Fig. 6. Quantile regression slope values (A) and intercept values (B) bounded by 95% CIs for cover and volume estimates for creosote and mesquite. Slope values of creosote and mesquite are not statistically different for volume estimates (mesquite: m = −1.14 ± 0.01; creosote: m = −1.15 ± 0.03), but are for cover estimates (mesquite: m = −1.16 ± 0.01; creosote: m = −1.20 ± 0.02). Intercept values for volume estimates are statistically different (mesquite: b = 6402 ± 303 m^3/patch; creosote: b = 7957 ± 1089 m^3/patch), as well as for cover estimates (mesquite: b = 7482 ± 325 m^2/patch; creosote: b = 9748 ± 1215 m^2/patch). Global slope and intercept values show the overall relationships (all species) with slope closer to −1 and reduced intercept due to the inclusion of additional sites with generally smaller and less dense plants.

(e.g., stem basal area vs diameter, canopy area vs volume), as well as differing focal species. Regardless, here we posited an expected thinning coefficient of −1 in the JRN-LTER based on previous work in savanna systems (Sea and Hanan 2012) and the logic that increases in the average size of plants in a community at carrying capacity must be attended by subsequent decreases in the number of plants so as not to exceed resource-limitations. We were then able to compare metrics of shrub size because an ideal structural metric will be directly proportional to resource use (i.e., thinning slope = −1). In our analysis, the integration of lidar-derived heights to index shrub volume in place of canopy area produced a thinning coefficient closer to our expectation, supporting our hypothesis that volume is a more appropriate index of woody plant size in drylands than canopy area. Importantly, shrub volume and shrub cover estimates were highly correlated (r = 0.929) due to an average shrub height of 1.08 m in the JRN-LTER. Although this correlation limits the value of height information in discerning thinning relationships, our results still suggest that lidar heights improve on canopy cover shrub size indices. However, canopy cover still performed well at quantifying thinning relationships and may be a viable alternative to lidar-based volume approaches where lidar data is limited.

When stratifying thinning results by species, creosote and mesquite populations occupy different portions of the volume-density feature space, with smaller but higher density stands being common in creosote locations, while lower density and larger shrubs are common in mesquite areas (Fig. 5). The smaller size, but higher density of creosote reflects the different morphology and growth patterns of these species (smaller and relatively dense creosote vs more spreading and often clonal mesquite; Duniway et al., 2018). This variation in morphology is likely due to differences in the functional strategies of creosote and mesquite (e.g., mesquite is a nitrogen-fixer while creosote is not), allowing both species to persist but through different pathways (Geesing et al., 2000). Regardless of their structural differences, both mesquite and creosote are well-modeled by the same thinning line (Fig. 5; Fig. 6), suggesting that the two species experience similar fundamental resource limitations and growth potential maxima. Furthermore, because thinning coefficients approximate −1, our results indicate that average shrub volume by density values (i.e., landscape scale shrub volume) are consistent across all size-classes. This theoretical upper bound on landscape-scale shrub volumes is the intercept of the thinning line quantile regression, which is 4084 m^3/ha for volume estimates in the JRN-LTER (Fig. 6).

Although the similar thinning slopes of creosote and mesquite suggest near-identical resource limitations, this does not imply that both species make use of limited water the same way. As precipitation is predicted to become more variable in the JRN-LTER (Bestelmeyer et al., 2015), the deep roots of mesquite may allow it to better withstand drought by accessing water resources inaccessible to creosote and other shrub species (Duniway et al., 2018; Meyer 1971). Due to this rooting morphology, mesquite likely has an advantage in areas with deep water sources (e.g., sandy soils), which may have long-term consequences on woody plant communities and hydrological processes in the JRN-LTER. Wilcox et al. (2022), for example, demonstrated increased surface runoff in arid regions undergoing WPE, especially in shrublands with bare inter-shrub spaces (e.g., mesquite shrubland). Therefore, the increased predominance of mesquite will likely impact important ecosystem services in arid regions such as groundwater recharge.

The thinning line illustrated in Fig. 5 identifies locations with high shrub size and density, which we assume corresponds with shrub carrying capacity constrained by local climate and edaphic conditions. The large number of sites below the thinning line, however, may reflect either local variation in carrying capacity, or local disequilibrium processes such as disturbance. Populations with lower carrying capacity might occur in sites where edaphic (topography, soils) or biotic factors (herbaceous competition) constrain or inhibit shrub growth (Archer et al., 2017; Greenland et al., 1997; Ji et al., 2019). Sites under disequilibrium, on the other hand, would be capable of supporting more shrubs, but do not due to processes limiting shrub establishment (e.g., drought or herbivory) or due to disturbances that increase shrub mortality (e.g., frost, or brush management activities). The combination of spatial heterogeneity in carrying capacity and bottlenecks to shrub establishment explains the abundance of sites below the thinning line in the JRN-LTER (Fig. 5). Our approach, however, is incapable of disentangling the causes of shrub populations occurring below the thinning line.

Ultimately, water underlies the thinning processes observed in the JRN-LTER. Evapo-transpiration greatly exceeds precipitation in the Chihuahuan Desert for most of the year (Wilcox et al., 2022), and parallel research shows that plant water use is more sensitive to neighborhood competition along a gradient of evaporative demand. These data therefore reinforce that water is the medium of competition in arid regions and increasing lateral root overlap and competition for soil water resources (rather than shrub volume or canopy cover, per se) is the mechanism limiting population growth rates at and near the thinning line (Wojcikiewicz et al., 2024). Though this remote sensing approach allows for inquiry at large spatial scales, assessments of competition and related thinning processes at individual scales may yield further insight into the controls on maximum shrub cover and mechanisms of shrub thinning in the JRN-LTER and the greater Chihuahuan Desert.

4.2. The importance of competition

Given the challenging environmental conditions of drylands, nurse plants and facilitative mechanisms are often considered important in the recruitment and growth of arid-adapted vegetation (Grünzweig et al., 2022). Our results do not dispute this importance, but reinforce that competition among shrubs in arid environments can occur even at relatively modest levels of canopy cover (~35% canopy cover at a density of 100 shrubs/ha in our study).

In the shrub encroachment literature, the “islands of fertility” concept has received significant attention (Schlesinger and Pilmanis 1998). “Islands of fertility” is not equivalent to woody plant encroachment but is a facilitative mechanism that is often critical in the early stages of encroachment. It refers to the heterogenous landscape of resource sparse and resource rich patches seen across recently encroached areas (Ridolfi et al., 2008). Our results may, therefore, be seen as an investigation into the natural conclusion of the encroachment process. If heterogenous patches of fertility facilitate encroachment, the eventual saturation of woody individuals leads to thinning and competitive limitation of population growth.

We propose an understanding of shrub encroachment as existing along a spectrum of facilitative and competitive interactions, with facilitation important in early stages and resource limitation and competition among woody plants important in later stages. Additional research is needed to understand competitive interactions among woody plants in post-encroached dryland systems, which may take on greater importance as woody plant encroachment continues to affect dryland ecosystems across the world.

Thinning relationships may even have potential as indices of shrub encroachment stages. Because thinning relationships should become stronger as encroachment progresses, the presence of thinning in an encroaching community suggests the increasing influence of competition. We suggest that post-encroachment shrub communities are typified by the increasing importance of competition compared to facilitation. Therefore, detection of highly competitive shrub communities via thinning lines provides a means to determine probable stages of encroachment. Implementation of this idea, however, requires additional research into the thinning dynamics of early and middle stages of woody plant encroachment.

4.3. Lidar in drylands

The use of USGS lidar to quantify shrub structure at large spatial-

scales (~100,000 ha) is novel to this study. We are unaware of any previous research using freely available USGS lidar for purposes besides forest and terrain mapping (Oh et al., 2022). However, unlike in forested systems, the implementation of USGS lidar in drylands is challenging and requires care (Kulawardhana et al., 2017). In particular, lidar-systems are limited by their ability to discriminate ground from vegetation (Ilangakoon et al., 2018). The USGS system used in this study, for example, has a minimum vertical resolution of 19.6 cm. In addition, terrain and vegetation properties, such as slope and leaf reflectance, can bias lidar-derived vegetation height estimates (Glenn et al., 2011).

Potential limitations in airborne lidar data notwithstanding, our methodology provided a reasonable compromise between leveraging USGS lidar for height estimates and accounting for its inadequacies by treating data as height samples. In particular, constraining height estimates to taller shrubs (>50 cm) and averaging height values from their native ~0.1/m^2 point density provided good averages at 1 ha scales. Although our 50 cm minimum height requirement excluded smaller and juvenile shrubs from our analysis, this exclusion likely had minimal impact on our results because our hypotheses focused on tall and dense shrub communities close to the thinning line. Still, we acknowledge that competition for limited resources in younger, smaller-sized shrub communities likely produces unique spatial patterns and may be important to shrub establishment and the propagation of WPE. Importantly, our shrub volume map was created by fusing estimates of canopy cover from multispectral NAIP data with the USGS lidar height data. It is possible that our fusion approach diluted information in the lidar height data with multispectral data, but this is unlikely because multiple other studies have demonstrated the value of data-fusion in producing estimates of vegetation structure (Bork and Su 2007). Therefore, we suggest that, while USGS lidar data may not fully resolve shrub populations in drylands, it provides useful data on hectare-scale heights that can be used to improve dryland vegetation structural retrievals when fused with high-resolution canopy cover data.

4.4. Additional research

Height data were not available to ground-truth our lidar-derived CHM. Instead, we relied on the verification completed by USGS, indicating a vertical accuracy of ~19.6 cm. Our 50 cm minimum height filter avoided inclusion of herbaceous vegetation, and averaging of height values to 1 ha scale increased confidence in mean shrub height estimates. We acknowledge, however, that future research, especially when measuring shrub heights below 50 cm or at finer scale than 1 ha, would benefit from formal verification.

Additional research into shrub community thinning will benefit from targeted experimental results. Here, we infer population-level processes (thinning) from observations of shrub size and density, but manipulation of density or underlying resources would yield more direct information. Direct observation of thinning processes, implemented via transplantation experiments or in natural populations, would provide insight into thinning processes, whether occurring through mortality of individuals or cessation of canopy growth. Direct observations may also provide information on thinning processes in species other than creosote or mesquite, including additional thinning strategies differing from those discussed here. Furthermore, because water ultimately constraints potential shrub size and density in drylands, direct measurement of plant water use using, for example, sap flow measurements, may provide further insight into the mechanisms of competition within the shrub populations of the JRN-LTER. Finally, improvements to lidar technology and publicly available data (e.g., from current NASA GEDI and ICESat-2 missions; Nazir et al., 2022) will refine estimates of shrub size in future analyses. For example, a similar approach to ours could implement improved lidar data (i.e., higher point density) by relaxing our 50 cm height threshold, analyzing shrub size at finer (<1 ha) scale, and including shrubs in the topographically rough areas excluded here. We expect improved LiDAR data products to further disentangle canopy cover and canopy volume estimates, which may decrease correlation between estimates and improve the application of volume measurements in remote-sensing community ecology studies.

5. Conclusion

We fused multispectral NAIP imagery and USGS lidar to quantify shrub size across a diverse landscape of contrasting soils and dominant shrub species in the semi-arid Jornada Basin of the Northern Chihuahuan Desert. Our results indicate that competition among shrubs (i.e., self-thinning) occurs at moderate density (~100 patches/ha) when canopy areas and volumes approach ~35%, with evidence that shrub canopy volumes provide a better index of shrub size and resource use than shrub canopy area. Dominant shrub species (i.e., mesquite vs. creosote) does not appear to alter the slope of thinning lines at the Jornada, suggesting that both creosote and mesquite populations experience the same fundamental constraints on their growth. The intense evaporative demand of the region implies that water limitation constraints shrub size and population density. By comparing shrub size maps to our expectations of thinning line coefficients, we conclude that fusing lidar-derived height data with NAIP-derived cover data produces better results than either dataset on its own. Future research will benefit from experimental manipulations that might include transplantation experiments to assess impacts of competition on seedling recruitment and adult growth rates, and direct measurements of plant water use (e.g., via sap flow) to measure changes in resource acquisition for plants growing in variable competitive neighborhoods.

CRediT authorship contribution statement

Trevor Roberts: Writing – original draft, Methodology, Formal analysis, Conceptualization. **Niall P. Hanan:** Writing – review & editing, Supervision, Conceptualization.

Declaration of competing interest

The authors declare the following financial interests/personal relationships which may be considered as potential competing interests:

Trevor Holden Roberts reports financial support was provided by Jornada Long-Term Ecological Research Program. Trevor Holden Roberts reports financial support was provided by New Mexico Space Grant Consortium. If there are other authors, they declare that they have no known competing financial interests or personal relationships that could have appeared to influence the work reported in this paper.

Data availability

Spatial and tabular data used in this article is available on EDI (https://doi.org/10.6073/pasta/49bec3ac2917e494c5de4b19130e703b).

Acknowldgement

This research was conducted on lands now known as the Jornada Basin which are the traditional homelands of the Piro, Tampachoa (Mansos) and Tiwa Peoples and the Mescalero Apache. The Chihuahuan Desert Rangeland Research Center is administered by New Mexico State University. Jornada Experimental Range is administered by the USDA-ARS. This work was supported by funding from the National Science Foundation to New Mexico State University for the Jornada Basin Long-Term Ecological Research Program (DEB 2025166). Support for TR was also provided *by the New Mexico Space* Grant *Consortium.*

References

Allred, B.W., Bestelmeyer, B.T., Boyd, C.S., Brown, C., Davies, K.W., Duniway, M.C., Ellsworth, L.M., Erickson, T.A., Fuhlendorf, S.D., Griffiths, T.V., Jansen, V., Jones, M. O., Karl, J., Knight, A., Maestas, J.D., Maynard, J.J., McCord, S.E., Naugle, D.E., Starns, H.D., Twidwell, D., Uden, D.R., 2021. Improving Landsat predictions of rangeland fractional cover with multitask learning and uncertainty. Methods Ecol. Evol. 12, 841–849. https://doi.org/10.1111/2041-210X.13564.

Archer, S.R., Andersen, E.M., Predick, K.I., Schwinning, S., Steidl, R.J., Woods, S.R., 2017. Woody plant encroachment: causes and consequences. In: Rangeland Systems. Springer, Cham, pp. 25–84.

Aschehoug, E.T., Brooker, R., Atwater, D.Z., Maron, J.L., Callaway, R.M., others, 2016. The mechanisms and consequences of interspecific competition among plants. Annual Review of Ecology. Evolution, and Systematics 47, 263–281.

Axelsson, C.R., Hanan, N.P., 2018. Rates of woody encroachment in African savannas reflect water constraints and fire disturbance. J. Biogeogr. 45, 1209–1218. https://doi.org/10.1111/jbi.13221.

Axelsson, C.R., Hanan, N.P., 2017. Patterns in woody vegetation structure across African savannas. Biogeosciences 14, 3239–3252. https://doi.org/10.5194/bg-14-3239-2017.

Belgrano, A., Allen, A.P., Enquist, B.J., Gillooly, J.F., 2002. Allometric scaling of maximum population density: a common rule for marine phytoplankton and terrestrial plants. Ecol. Lett. 5, 611–613.

Bestelmeyer, B.T., Okin, G.S., Duniway, M.C., Archer, S.R., Sayre, N.F., Williamson, J.C., Herrick, J.E., 2015. Desertification, land use, and the transformation of global drylands. Front. Ecol. Environ. 13, 28–36.

Black, K.L., Wallace, C.A., Baltzer, J.L., 2021. Seasonal thaw and landscape position determine foliar functional traits and whole-plant water use in tall shrubs on the low arctic tundra. New Phytol. 231, 94–107.

Bork, E.W., Su, J.G., 2007. Integrating LIDAR data and multispectral imagery for enhanced classification of rangeland vegetation: a meta analysis. Rem. Sens. Environ. 111, 11–24. https://doi.org/10.1016/j.rse.2007.03.011.

Buffington, L.C., Herbel, C.H., 1965. Vegetational changes on a semidesert grassland range from 1858 to 1963. Ecol. Monogr. 35, 140–164. https://doi.org/10.2307/1948415.

Carrasco, L., Giam, X., Papeş, M., Sheldon, K.S., 2019. Metrics of lidar-derived 3D vegetation structure reveal contrasting effects of horizontal and vertical forest heterogeneity on bird species richness. Rem. Sens. 11 https://doi.org/10.3390/rs11070743.

Christensen, E., James, D., Maxwell, C.J., Slaughter, A., Adler, P.B., Havstad, K., Bestelmeyer, B., 2021. Quadrat-based monitoring of desert grassland vegetation at the Jornada Experimental Range, New Mexico, 1915–2016. Ecology 102, e03530. https://doi.org/10.1002/ecy.3530.

Craine, J.M., Dybzinski, R., 2013. Mechanisms of plant competition for nutrients, water and light. Funct. Ecol. 27, 833–840.

D'Odorico, P., Okin, G.S., Bestelmeyer, B.T., 2012. A synthetic review of feedbacks and drivers of shrub encroachment in arid grasslands. Ecohydrology 5, 520–530. https://doi.org/10.1002/eco.259.

Dohn, J., Augustine, D.J., Hanan, N.P., Ratnam, J., Sankaran, M., 2017. Spatial vegetation patterns and neighborhood competition among woody plants in an East African savanna. Ecology 98, 478–488.

Duniway, M.C., Petrie, M.D., Peters, D.P., Anderson, J.P., Crossland, K., Herrick, J.E., 2018. Soil water dynamics at 15 locations distributed across a desert landscape: insights from a 27-yr dataset. Ecosphere 9, e02335.

Ge, F., Zeng, W., Ma, W., Meng, J., 2017. Does the slope of the self-thinning line remain a constant value across different site qualities?—an implication for plantation density management. Forests 8. https://doi.org/10.3390/f8100355.

Geesing, D., Felker, P., Bingham, R.L., 2000. Influence of mesquite (Prosopis glandulosa) on soil nitrogen and carbon development: implications for global carbon sequestration. J. Arid Environ. 46, 157–180. https://doi.org/10.1006/jare.2000.0661.

Gibbens, R., McNeely, R., Havstad, K., Beck, R., Nolen, B., 2005. Vegetation changes in the Jornada Basin from 1858 to 1998. J. Arid Environ. 61, 651–668.

Glenn, N.F., Spaete, L.P., Sankey, T.T., Derryberry, D.R., Hardegree, S.P., Mitchell, J.J., 2011. Errors in LiDAR-derived shrub height and crown area on sloped terrain. J. Arid Environ. 75, 377–382. https://doi.org/10.1016/j.jaridenv.2010.11.005.

Goslee, S.C., Havstad, K.M., Peters, D.P.C., Rango, A., Schlesinger, W.H., 2003. High-resolution images reveal rate and pattern of shrub encroachment over six decades in New Mexico, U.S.A. J. Arid Environ. 54, 755–767. https://doi.org/10.1006/jare.2002.1103.

Greenland, D., Kittel, T., Hayden, B., Schimel, D., 1997. A climatic analysis of long-term ecological research sites. See. http://intranet2.lternet.edu/sites/intranet2.lternet.edu/files/documents/Scientific/20Reports/Climate/20and/20Hydrology/20Database/20Projects/CLIMDES.pdf.

Grünzweig, J.M., De Boeck, H.J., Rey, A., Santos, M.J., Adam, O., Bahn, M., Belnap, J., Deckmyn, G., Dekker, S.C., Flores, O., others, 2022. Dryland mechanisms could widely control ecosystem functioning in a drier and warmer world. Nature Ecology & Evolution 6, 1064–1076.

Hatton, I.A., Dobson, A.P., Storch, D., Galbraith, E.D., Loreau, M., 2019. Linking Scaling Laws across Eukaryotes, vol. 116. Proceedings of the National Academy of Sciences, pp. 21616–21622.

Havstad, K.M., Huenneke, L.F., Schlesinger, W.H., 2006. Structure and Function of a Chihuahuan Desert Ecosystem: the Jornada Basin Long-Term Ecological Research Site. Oxford University Press.

Hijmans, R.J., 2022. Terra: Spatial Data Analysis.

Huang, C., Archer, S.R., McClaran, M.P., Marsh, S.E., 2018. Shrub encroachment into grasslands: end of an era? PeerJ 6, e5474.

Huang, J., Li, Y., Fu, C., Chen, F., Fu, Q., Dai, A., Shinoda, M., Ma, Z., Guo, W., Li, Z., others, 2017. Dryland climate change: Recent progress and challenges. Rev. Geophys. 55, 719–778.

Ilangakoon, N.T., Glenn, N.F., Dashti, H., Painter, T.H., Mikesell, T.D., Spaete, L.P., Mitchell, J.J., Shannon, K., 2018. Constraining plant functional types in a semi-arid ecosystem with waveform lidar. Rem. Sens. Environ. 209, 497–509. https://doi.org/10.1016/j.rse.2018.02.070.

Ji, W., Hanan, N.P., Browning, D.M., Monger, H.C., Peters, D.P.C., Bestelmeyer, B.T., Archer, S.R., Ross, C.W., Lind, B.M., Anchang, J., Kumar, S.S., Prihodko, L., 2019. Constraints on shrub cover and shrub-shrub competition in a U.S. southwest desert. Ecosphere 10. https://doi.org/10.1002/ecs2.2590.

Jones, M.O., Robinson, N.P., Naugle, D.E., Maestas, J.D., Reeves, M.C., Lankston, R.W., Allred, B.W., 2021. Annual and 16-Day Rangeland Production Estimates for the Western United States. Rangel. Ecol. Manag. 77, 112–117. https://doi.org/10.1016/j.rama.2021.04.003.

Koenker, R., 2022. Quantreg: Quantile Regression.

Kulawardhana, R.W., Popescu, S.C., Feagin, R.A., 2017. Airborne lidar remote sensing applications in non-forested short stature environments: a review. Ann. For. Res. 60, 173–196.

Liu, F., Song, Q., Zhao, J., Mao, L., Bu, H., Hu, Y., Zhu, X.-G., 2021. Canopy occupation volume as an indicator of canopy photosynthetic capacity. New Phytol. 232, 941–956. https://doi.org/10.1111/nph.17611.

Maestre, F.T., Eldridge, D.J., Soliveres, S., Kéfi, S., Delgado-Baquerizo, M., Bowker, M.A., García-Palacios, P., Gaitán, J., Gallardo, A., Lázaro, R., others, 2016. Structure and functioning of dryland ecosystems in a changing world. Annu. Rev. Ecol. Evol. Syst. 47, 215.

Meyer, R.E., 1971. Morphology and Anatomy of Honey Mesquite. US Department of Agriculture.

Nazir, A., Yu, Q., Prihodko, L., Roberts, T.H., Hanan, N.P., 2022. Assessing the Accuracy of GEDI Cover in arid and semiarid regions of New Mexico, USA. In: AGU Fall Meeting Abstracts, pp. B45H–B1809.

Oh, S., Jung, J., Shao, Guofan, Shao, Gang, Gallion, J., Fei, S., 2022. High-resolution canopy height model generation and validation using usgs 3dep lidar data in indiana, usa. Rem. Sens. 14, 935.

Pebesma, E., 2021. Stars: Spatiotemporal Arrays, Raster and Vector Data Cubes.

Pebesma, E., 2018. Simple Features for R: Standardized Support for Spatial Vector Data. RELC J. 10, 439–446. https://doi.org/10.32614/RJ-2018-009.

Peters, D.P., Gibbens, R.P., 2006. Plant communities in the Jornada Basin: the dynamic landscape. Structure and Function of a Chihuahuan Desert Ecosystem: the Jornada Basin Long-Term Ecological Research Site, pp. 211–231.

R Core Team, 2021. R: A Language and Environment for Statistical Computing. R Foundation for Statistical Computing, Vienna, Austria.

Reid, R.S., Fernández-Giménez, M.E., Galvin, K.A., others, 2014. Dynamics and resilience of rangelands and pastoral peoples around the globe. Annu. Rev. Environ. Resour. 39, 217–242.

Ridolfi, L., Laio, F., D'Odorico, P., 2008. Fertility island formation and evolution in dryland ecosystems. Ecol. Soc. 13.

Roberts, T.H., Hanan, N.P., 2023. Gridded 1-hectare Estimates of Shrub Community Structure at the Jornada Basin LTER Site Derived from NAIP (2011) and LiDAR, 10.6073, (2019).

Roussel, J.-R., Auty, D., Coops, N.C., Tompalski, P., Goodbody, T.R.H., Meador, A.S., Bourdon, J.-F., Boissieu, F. de, Achim, A., 2020. lidR: An R package for analysis of Airborne Laser Scanning (ALS) data. Rem. Sens. Environ. 251, 112061 https://doi.org/10.1016/j.rse.2020.112061.

Saco, P.M., Moreno-de las Heras, M., Keesstra, S., Baartman, J., Yetemen, O., Rodríguez, J.F., 2018. Vegetation and soil degradation in drylands: non linear feedbacks and early warning signals. Current Opinion in Environmental Science & Health 5, 67–72.

Sayre, N.F., deBuys, W., Bestelmeyer, B.T., Havstad, K.M., 2012. "The Range Problem" After a Century of Rangeland Science: New Research Themes for Altered Landscapes. Rangel. Ecol. Manag. 65, 545–552. https://doi.org/10.2111/REM-D-11-00113.1.

Schlesinger, W.H., Pilmanis, A.M., 1998. Plant-soil Interactions in Deserts. Biogeochemistry 42, 169–187. https://doi.org/10.1023/A:1005939924434.

Schmidt-Walter, P., Richter, F., Herbst, M., Schuldt, B., Lamersdorf, N.P., 2014. Transpiration and water use strategies of a young and a full-grown short rotation coppice differing in canopy cover and leaf area. Agric. For. Meteorol. 195–196, 165–178. https://doi.org/10.1016/j.agrformet.2014.05.006.

Sea, W.B., Hanan, N.P., 2012. Self-thinning and tree competition in savannas. Biotropica 44, 189–196.

Stockle, C.O., 1992. Canopy photosynthesis and transpiration estimates using radiation interception models with different levels of detail. Ecol. Model. 60, 31–44. https://doi.org/10.1016/0304-3800(92)90011-3.

Taki, H., Inoue, T., Tanaka, H., Makihara, H., Sueyoshi, M., Isono, M., Okabe, K., 2010. Responses of community structure, diversity, and abundance of understory plants and insect assemblages to thinning in plantations. For. Ecol. Manag. 259, 607–613. https://doi.org/10.1016/j.foreco.2009.11.019.

Urgoiti, J., Messier, C., Keeton, W.S., Belluau, M., Paquette, A., 2023. Functional diversity and identity influence the self-thinning process in young forest communities. J. Ecol. 111, 2010–2022. https://doi.org/10.1111/1365-2745.14158.

Vospernik, S., Sterba, H., 2015. Do competition-density rule and self-thinning rule agree? Ann. For. Sci. 72, 379–390.

West, G.B., Brown, J.H., Enquist, B.J., 1999. The fourth dimension of life: fractal geometry and allometric scaling of organisms. Science 284, 1677–1679.

Wickham, H., Averick, M., Bryan, J., Chang, W., McGowan, L.D., François, R., Grolemund, G., Hayes, A., Henry, L., Hester, J., Kuhn, M., Pedersen, T.L., Miller, E., Bache, S.M., Müller, K., Ooms, J., Robinson, D., Seidel, D.P., Spinu, V., Takahashi, K., Vaughan, D., Wilke, C., Woo, K., Yutani, H., 2019. Welcome to the tidyverse. J. Open Source Softw. 4, 1686. https://doi.org/10.21105/joss.01686.

Wilcox, B.P., Basant, S., Olariu, H., Leite, P.A., 2022. Ecohydrological connectivity: A unifying framework for understanding how woody plant encroachment alters the water cycle in drylands. Front. Environ. Sci. 10.

Wojcikiewicz, R., Ji, W., Hanan, N.P., 2024. Quantifying shrub–shrub competition in drylands using aerial imagery and a novel landscape competition index. New Phytol. 241, 1973–1984. https://doi.org/10.1111/nph.19505.

Yu, K., Chen, H.Y.H., Gessler, A., Pugh, T.A.M., Searle, E.B., Allen, R.B., Pretzsch, H., Ciais, P., Phillips, O.L., Brienen, R.J.W., Chu, C., Xie, S., Ballantyne, A.P., 2024. Forest demography and biomass accumulation rates are associated with transient mean tree size vs density scaling relations. PNAS Nexus pgae008. https://doi.org/10.1093/pnasnexus/pgae008.